Progress In Electromagnetics Research, Vol. 123, 143–158, 2012

STUDY OF AN EXTREMELY WIDEBAND MONOPOLE ANTENNA WITH TRIPLE BAND-NOTCHED CHARACTERISTICS

J. Liu[1, 2, *], K. P. Esselle[1], S. G. Hay[2], and S. S. Zhong[3]

[1]Centre for Microwave and Wireless Applications, Electronic Engineering, Macquarie University, Sydney, NSW 2109, Australia

[2]CSIRO, ICT Centre, P. O. Box 76, Epping Sydney, NSW 1710, Australia

[3]School of Communication and Information Engineering, Shanghai University, Shanghai 200072, China

Abstract—Three notched bands are generated, at selected frequencies, in an extremely wideband base antenna to support multiple communication systems while avoiding inference from other existing narrowband systems. The design of a fully printed extremely wideband antenna and creating triple band-notched functions are addressed in this paper. Measurements demonstrate that the proposed printed base antenna has an extremely wide 2 : 1 VSWR bandwidth from 0.72 GHz, to 25 GHz with a ratio bandwidth of 34 : 1. The antenna has a simple structure and can be fabricated at low cost for multi-band and wideband wireless communication devices. Besides, this paper presents a technique to form three notched bands within the operating frequency range of the base antenna. By introducing a half-wavelength U-shaped defected ground structure (DGS) and a pair of quarter-wavelength open arc-shaped slots to the radiating patch, three notched bands are created to prevent interference from WLAN (2.4–2.484 GHz and 5.15–5.85 GHz) systems and downlinks of X-band satellite communication (7.25–7.75 GHz) systems.

Received 4 November 2011, Accepted 5 December 2011, Scheduled 18 December 2011
* Corresponding author: Jianjun Liu (jianjun@science.mq.edu.au).

1. INTRODUCTION

The Federal Communication Commission's (FCC) allocation of 3.1 to 10.6 GHz for ultra-wideband (UWB) communication has created interest in antennas with ultra or extremely wide bandwidths. For UWB systems, printed monopole antennas with various radiation patch shapes are widely used due to their advantages of low cost, light weight and ease of fabricating and integrating with electronic devices [1–9]. In order to support multiple communication services in a single device through UWB and other communication systems, a single antenna that has the ability to operate in all these frequency bands is highly desirable. Printed antenna designs with enhanced bandwidths for multiple wireless systems have been proposed recently. For example, in [10], a printed elliptical monopole antenna with a hexagonal ground plane has been introduced to support UMTS and UWB systems. A microstrip-fed antenna with an L-shaped ramification on the radiation patch has been presented in [11] for Bluetooth and UWB systems. In our lab, a printed elliptical antenna with a tapered and modified feed was designed to support a number of wireless communication frequency bands [12].

On the other hand, within the FCC-designated band for UWB systems, there exist several relatively narrow frequency bands used by other wireless systems such as IEEE 802.11b/g/n wireless local-area networks (WLAN) operating at 2.4–2.484 GHz, IEEE 802.11a/n operating at 5.15–5.35 GHz and 5.725–5.825 GHz and downlink of X-band satellite communication systems operating at 7.25–7.75 GHz. To avoid interference between UWB systems and these narrowband wireless communication systems, separate bandnotch filters can be added to the system. However, these additional filters will increase the volume, weight and complexity of the system. Recently, many wideband antennas with integrated band-notched functions have been developed, to avoid the need for external bandnotch filters. It has been achieved by embedding complementary resonant elements into the main radiating element. For example, slots of various shapes made in a radiation patch can provide such a band-notched function [13–23]. However, these slot layouts can provide only one notched bands, and hence their practical applications are limited. Recently, some designs with the characteristics of a dual notched band [24–33] and even a triple notched band are presented [34–36].

An extremely wideband antenna with three notched bands is presented in this paper. It is organized as follows. Section 2 describes the base antenna, which has an extremely wide bandwidth. The measured results indicate that the bandwidth of the base

antenna ranges from 0.72 GHz to 25 GHz with a ratio bandwidth of 34 : 1. Hence, it can support many communication systems such as GSM (880–960 MHz), GPS (1.57–1.58 GHz),WCDMA (1.92–2.17 GHz), UWB (3.1–10.6 GHz) and MVDDS (12.2–12.7 GHz). The principle of its operation is also studied. Section 3 describes the triple band-notched functions, which are realized on this extremely wideband printed antenna. Three notched bands are achieved by introducing a half-wavelength U-shaped defected ground structure (DGS) and a pair of quarter-wavelength open arc-shaped slots. The variation of the slots and DGS parameters on multiple band-notched functions are discussed. The principles of the band-notched design are also presented with formulas in this paper.

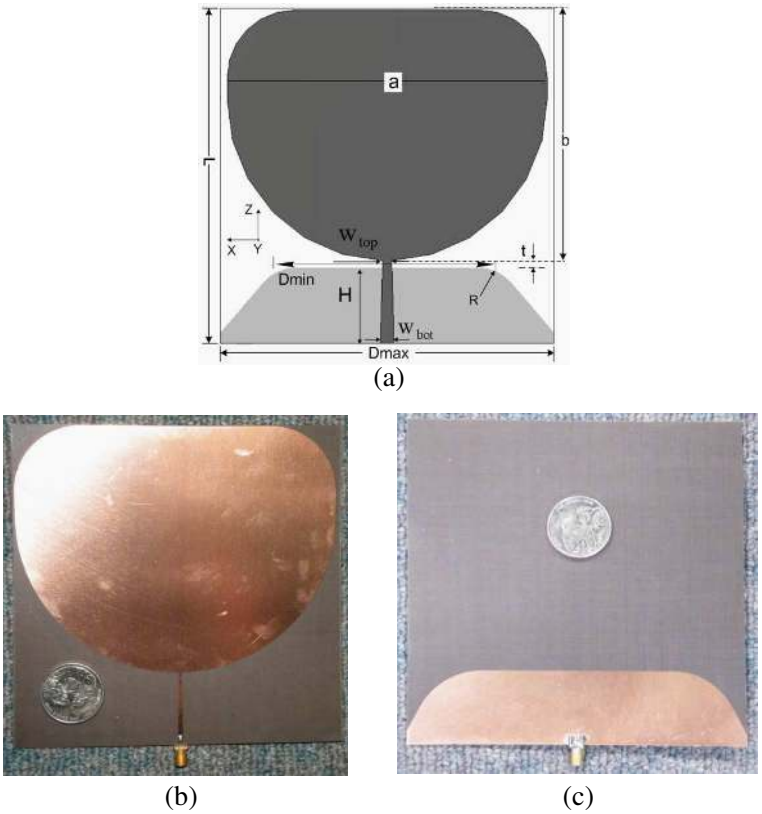

Figure 1. (a) The configuration of the base antenna. (b) The top side of the fabricated base antenna. (c) The back side of the fabricated base antenna.

2. BASE ANTENNA DESIGN

The base antenna is composed of a printed monopole and a modified trapezoid ground plane, illustrated in Figure 1(a). The ground plane and monopole are etched on the back and top surfaces of a TACONIC TLX-0 substrate, respectively. Its thickness (h) is 0.787 mm, the relative permittivity (ε_r) 2.45 and the metal cladding thickness 0.01 mm. The monopole, with maximum length a and width b, is fed by a tapered microstrip feeding line in the middle of the ground plane. The ground plane is a part of the impedance matching network. The top rounded corners of the trapezoid ground plane reduce the sensitivity to fabrication tolerances and help to achieve a better impedance match. The radius of the rounded bends of the ground plane is denoted by R. The gap, t, between the patch and the trapezoidal ground plane, plays a vital role in bandwidth performance. The width of the central strip at the top end (W_{top}) is 1.1 mm, corresponding to a characteristic impedance of 75 Ω, and the width at the bottom end (W_{bot}) is 2.3 mm, corresponding to a characteristic impedance of 50 Ω. The tapered feeding line gradually transforms the impedance from 50 to 75 Ω and provides better wideband performance than a

Table 1. Dimensions of the base antenna [mm].

$\mathbf{D}_{\text{max}}$	$\mathbf{D}_{\text{min}}$	**H**	**t**	$\mathbf{W}_{\text{top}}$
150	120	34	0.4	1.1
a	**b**	**L**	**R**	$\mathbf{W}_{\text{bot}}$
144	114	150	25	2.3

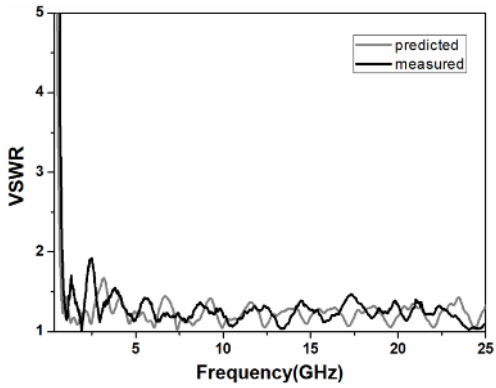

Figure 2. Measured and predicted VSWR of the base antenna.

straight microstrip feed. Parametric analyses of this base antenna have been conducted by changing one parameter at a time while keeping the others constant. Through proper selection of the parameters of the ground plane and radiation patch, a greatly enhanced impedance bandwidth can be achieved. The selected parameter values are listed in Table 1. The photograph of the fabricated antenna is shown in Figures 1(b) and (c).

The base antenna has been designed and optimised using CST Microwave Studio commercial software, and the measured VSWR results have been obtained by using a Wiltron37369A vector network analyser (40 MHz–40 GHz). The predicted 2 : 1 VSWR bandwidth is from 0.705 to 25 GHz, while the measured bandwidth covers a

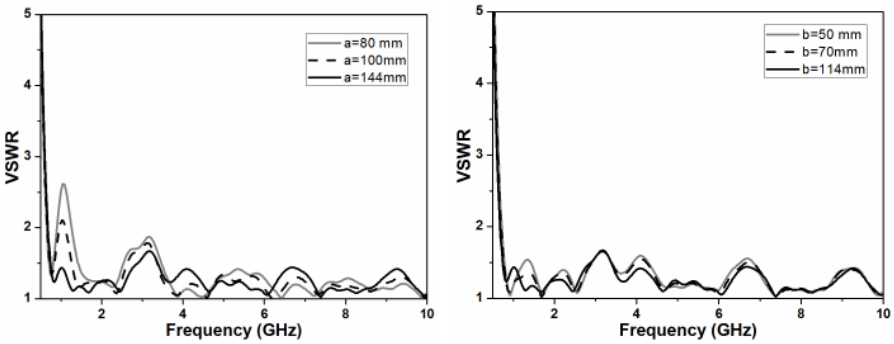

Figure 3. VSWR of the base antenna with different patch (a) widths a and (b) lengths b.

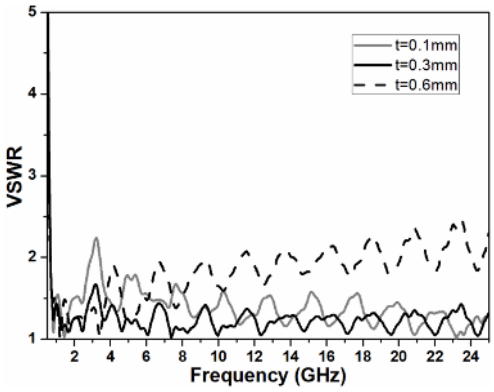

Figure 4. VSWR of antennas with different gaps.

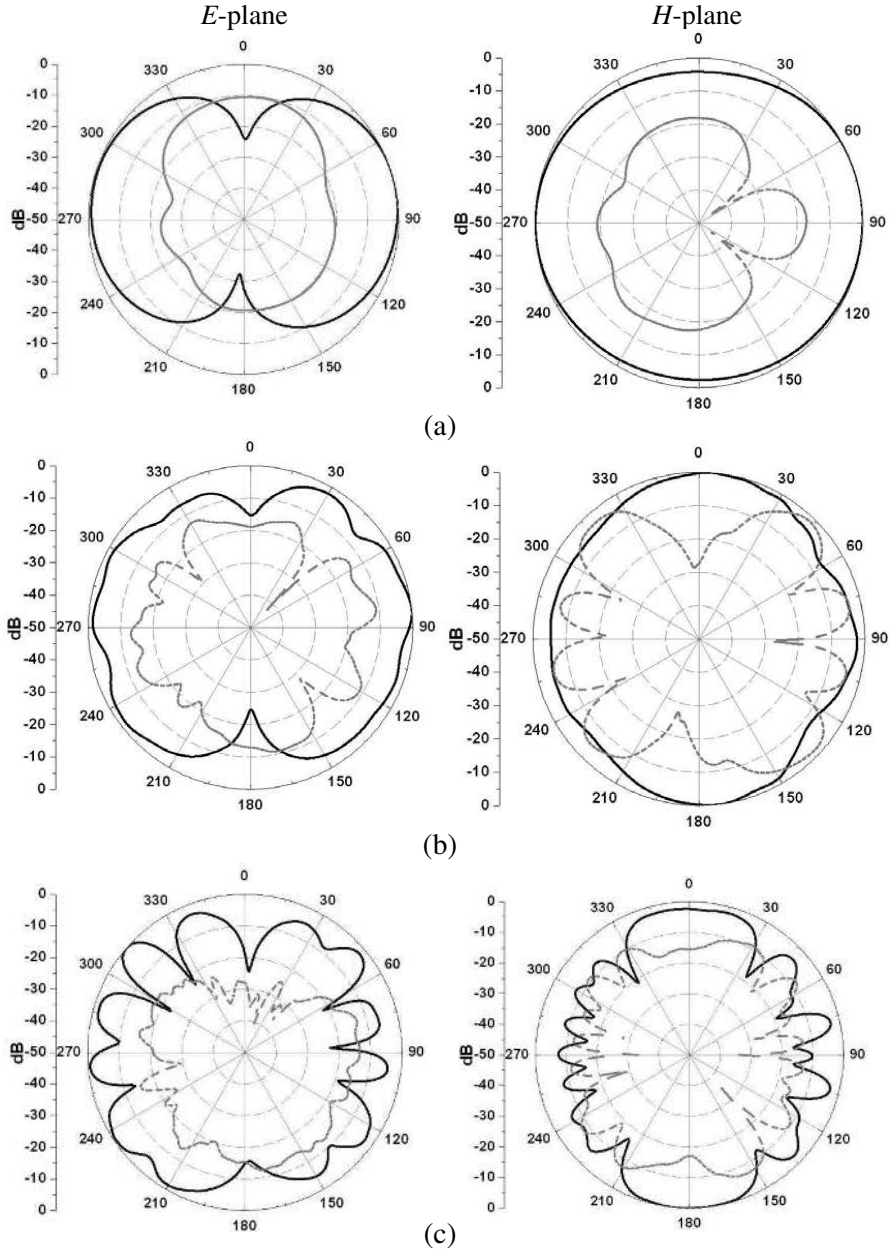
E-plane
H-plane
dB
0
-10
-20
-30
-40
-50
30
60
90
120
150
180
210
240
270
300
330
(a)
(b)
(c)

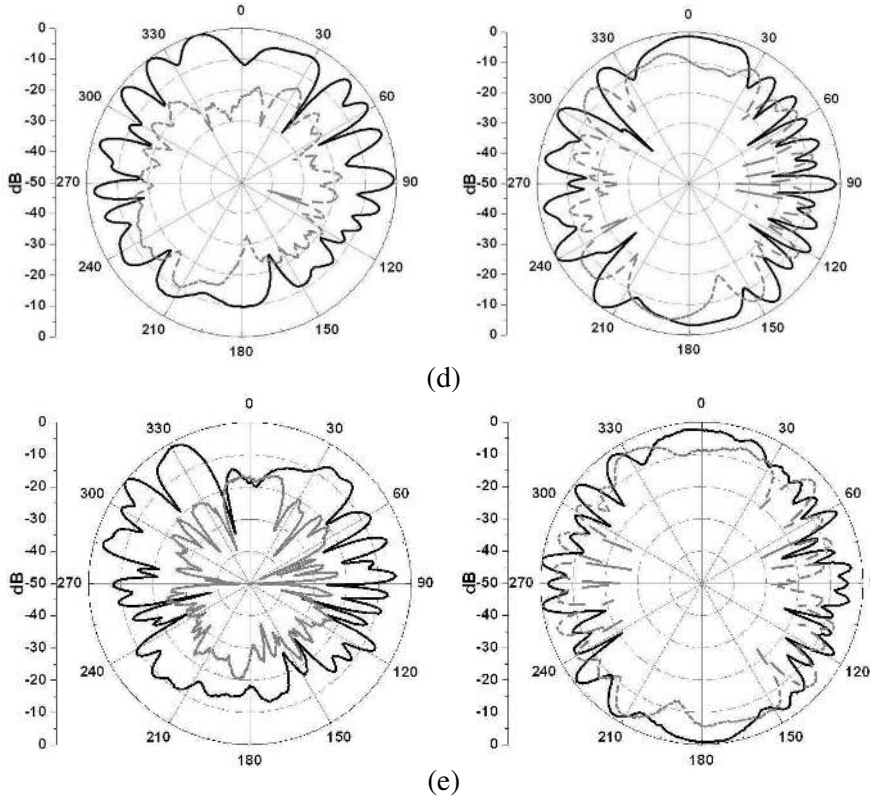

Figure 5. Measured radiation patterns. (a) $f = 1\,\text{GHz}$. (b) $f = 5\,\text{GHz}$. (c) $f = 10\,\text{GHz}$. (d) $f = 15\,\text{GHz}$. (e) $f = 20\,\text{GHz}$.

frequency range from 0.72 to 25 GHz with a ratio bandwidth of 34 : 1 (see Figure 2). A good agreement between the predicted and measured results can be observed. The low frequency limit of the VSWR bandwidth is determined by the total effective length of the antenna current path, which includes the radiation patch and the ground plane. Therefore, increasing the effective dimensions of the radiation patch and ground plane can decrease the low frequency limit. As shown in Figure 3, when the patch width a is increased from 80 to 144 mm, the lower frequency limit decreases from 1.43 GHz to 0.705 GHz. The lower frequency limit is reduced from 0.84 GHz to 0.705 GHz when the patch height b is increased from 50 mm to 144 mm. The higher frequency limit is associated with several parameters, including the gap between the patch and the trapezoid ground plane and the microstrip to monopole terminal layout. Figure 4 indicates that the impedance matching at

high frequencies strongly depends on the gap t.

The measured normalized far-field radiation patterns at 1, 5, 10, 15 and 20 GHz are shown in Figure 5. They indicate that this antenna has a nearly omni-directional radiation pattern at low frequencies in the H-plane (e.g., at 1 GHz). The E-plane radiation pattern shows two nulls at 1 GHz, which is similar to that of a conventional dipole antenna. The cross polarization on the E-plane stays at relatively low levels over the whole operating frequency band. However, in the H-plane, it can be seen that the cross-polarization level rises with frequency owing to the increasing horizontal component of surface currents. Pattern ripples become more prominent at higher frequencies since the antenna operates in higher order modes instead of the typical monopole mode.

3. CREATING TRIPLE NOTCHED BANDS

In this section, to avoid potential interference with 802.11a/b/g/n WLAN systems and downlink of X-band satellite communication systems, band notching is introduced to the base antenna described in Section 2. This is achieved by embedding a defected ground structure (DGS) and arc-shaped slots that resonate around notched bands. The configuration of the antenna with triple notched bands is illustrated in Figure 6. As shown in Figure 6(a), a pair of arc-shaped open slots is symmetrically positioned on the radiation patch to achieve

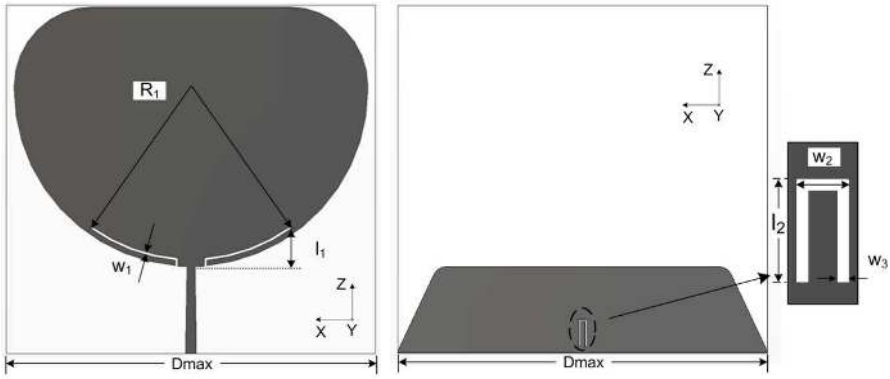

Figure 6. The configuration of the triple band-notched antenna. (a) Top side. (b) Back side ($l_1 = 5.5$ mm, $l_2 = 10.5$ mm, $w_1 = 0.3$ mm, $w_2 = 1.0$ mm, $w_3 = 0.3$ mm, $R_1 = 65$ mm).

notched bands with central frequencies around 2.4 GHz and 7.5 GHz. The widths of the arc-shaped slots are 0.3 mm. To produce a notched band around 5.5 GHz, a U-shaped DGS has been formed in the ground plane, as shown in the insert of Figure 6(b). The DGS has a width of w_3 and a length of l_2. The distance between the two slots of the DGS is w_2. Compared with the slots on the radiation patch, the U-shaped DGS produces lesser horizontal surface currents and prevents high cross polarization in other operating frequencies of the antenna. The parameter values of the band-notched antenna design are listed in the caption of Figure 6.

Figure 7 shows the photograph of an antenna prototype with the

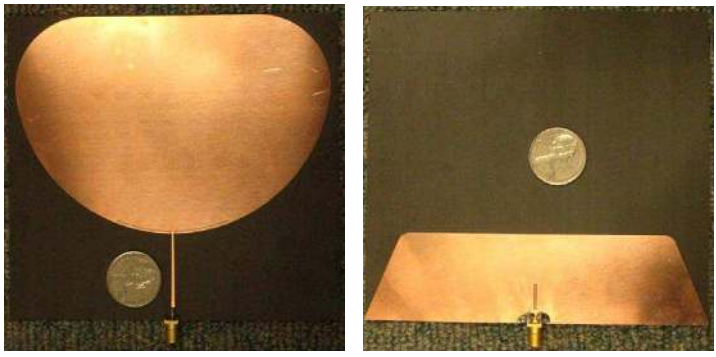

(a) (b)

Figure 7. Photograph of the fabricated triple band-notched antenna. (a) Top side. (b) Back side.

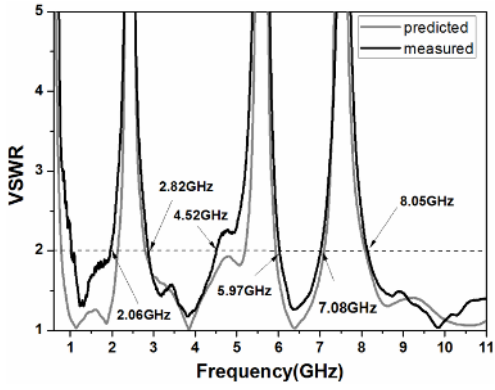

Figure 8. VSWR of the antenna with three notched bands.

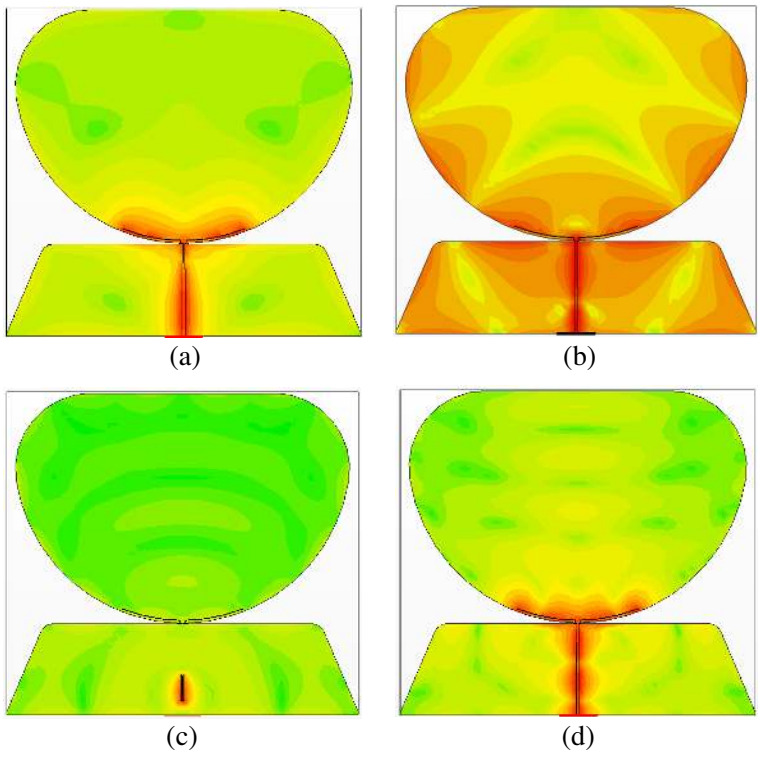

Figure 9. Surface current distributions at four different frequencies. (a) Top side at 2.4 GHz (within the first notched band). (b) Top side at 4 GHz (passband). (c) Back side at 5.5 GHz (within the second notched band). (d) Top side at 7.5 GHz (within the third notched band).

triple band-notched function. The predicted and measured VSWR curves of this antenna are illustrated in Figure 8. The antenna displays wideband performance with three notched bands in the frequency ranges of 2.06–2.82 GHz, 4.52–5.97 GHz and 7.08–8.05 GHz. The predicted result agrees well with the measured one. The triple notched bands successfully avoid interference from 802.11a/b/g WLAN systems (2.4–2.484 GHz and 5.15–5.85 GHz) and downlink of X-band satellite communication systems (7.25–7.75 GHz).

To gain a better understanding of the antenna operation, the surface current distributions at four different frequencies of 2.4 GHz, 4 GHz, 5.5 GHz and 7.5 GHz are presented in Figure 9. These frequencies correspond to the centers of the three notched bands and one passband. At the notch frequencies, the strongest electric currents

exist around the slot that resonates in this band while there is very weak current flow within the interior of the monopole, as can be seen in Figures 9(a) and (c). At the passband frequency of 4 GHz, the surface current distribution is more uniform than that at notched frequencies, as shown in Figure 9(b). In Figure 9(d), the current distribution concentrates around the edge of the arc-shaped slots again, which confirms that the arc-slot pair also resonates at 7.5 GHz. Its first-order resonance is around 2.4 GHz and the third-order resonance is around 7.5 GHz. By properly placing the arc-shaped slots, two notched bands have been generated by only one set of slots, simplifying the antenna configuration.

The band-notched characteristics produced by the arc-shaped slots and U-shaped DGS are investigated below. The relationship between the resonance frequency and the length of the arc-shaped slots is given by

$$f_{\text{arc}} = \frac{c}{4l_{\text{arc}}\sqrt{\varepsilon_{eff}}} \tag{1}$$

where l_{arc} is the length of the arc-shaped slots, c the speed of light, and ε_{eff} the effective dielectric constant.

The relationship between the resonance frequency and the length of the U-shaped DGS is given by

$$f_U = \frac{c}{2l_U\sqrt{\varepsilon_{eff}}} \tag{2}$$

where l_U is the length of the DGS. Ideally, the central frequencies of the notched bands are determined by the lengths of the U-shaped DGS or the arc-shaped slot. Nevertheless, the location of the DGS or the arc-shaped slot on the antenna also slightly affects the center frequencies

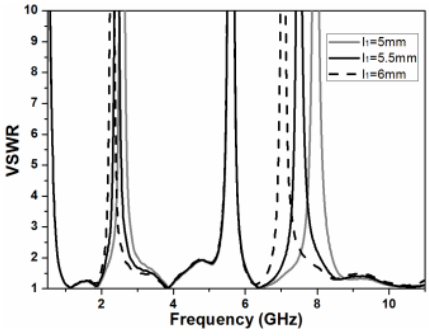

Figure 10. VSWR for various slot lengths l_1.

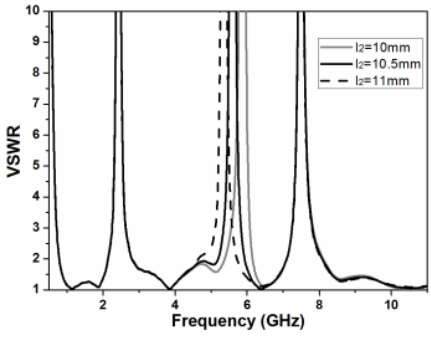

Figure 11. VSWR for various DGS slot lengths l_2.

of the notched bands. Therefore, the above formulas have been used to obtain initial design parameters for the resonant elements. These parameters have been optimized later with Microwave Studio full-wave simulations.

As shown in Figures 10 and 11, with the increasing lengths of the arc-shaped slots and the U-shaped DGS, the central frequency of each notched band decreases. Furthermore, the proposed antenna has quite stable band-notched characteristics. Although the notches shift with the tuning of the corresponding resonant element, the characteristics of the other notched bands remain steady. Figure 12 shows the sensitivity of the antenna VSWR to the width of the arc-shaped slot. When the width is increased from 0.1 to 0.3 mm, the 2.4 GHz notched band (VSWR $\geq$ 2) becomes wider, from 350 to 520 MHz, and the 7.5 GHz notched band also becomes wider, from 600 to 1150 MHz. Figure 13

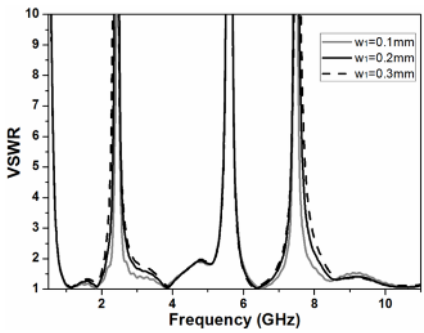

Figure 12. VSWR for various widths w_1.

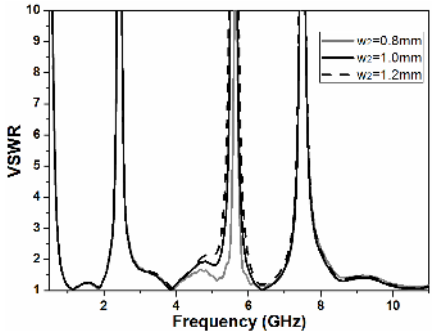

Figure 13. VSWR for various DGS slot spacings w_2.

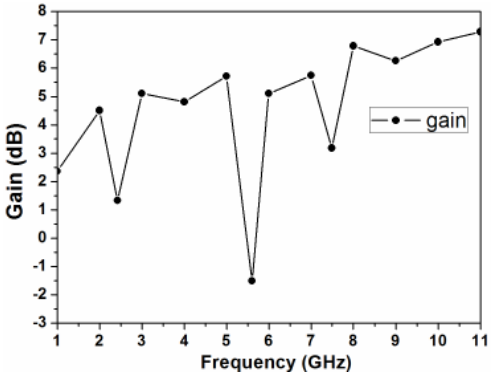

Figure 14. Measured gain of the antenna with three notched bands.

shows how the antenna VSWR depends on the spacing between the two DGS slots. A wider notched band can be observed from 710 to 1260 MHz, when the spacing is increased from 0.8 to 1.2 mm. These results indicate that the bandwidth of the notches can be adjusted by altering the shapes and width of the slots.

Figure 14 displays the measured gain of the antenna with multiple notched bands. Between 1 GHz and 11 GHz, three significant drops of the gain can be observed. The frequencies of the minima correspond to the center frequencies of the notched bands. These results confirm the expected suppression of radiation in the notched frequency bands.

4. CONCLUSION

Three notched bands have been created within the operating bandwidth of a printed extremely wideband antenna, which otherwise has a continuous measured 2 : 1 VSWR bandwidth from 0.72 GHz to more than 25 GHz. This is achieved by introducing a DGS and two open arc-shaped slots. The notches have been tuned to prevent interference from WLAN (both 2.4 and 5.5 GHz) bands and downlink X-band satellite communication systems (7.5 GHz). The performance of the proposed antenna has been investigated. Due to its extremely wide bandwidth, it can support multiple communication services while avoiding interference from other selected systems.

ACKNOWLEDGMENT

This work has been supported by the Australian Research Council, the Shanghai Leading Academic Discipline Project under Grant No. S30108, Macquarie University Research Excellence Scholarship (MQRES) scheme and CSIRO Postgraduate Scholarship.

REFERENCES

1. Zhang, Z. and Y. H. Lee, "A robust cad tool for integrated design of UWB antenna system," *Progress In Electromagnetics Research*, Vol. 112, 441–457, 2011.
2. Jiang, W., T. Hong, Y. Liu, S.-X. Gong, Y. Guan, and S. Cui, "A novel technique for radar cross section reduction of printed antennas," *Journal of Electromagnetic Waves and Applications*, Vol. 24, No. 1, 51–60, 2010.

3. Dissanayake, T., K. P. Esselle, and Y. H. Ge, "A printed triangular-ring antenna with a 2 : 1 bandwidth," *Microwave Opt. Tech. Lett.*, Vol. 44, No. 1, 51–53, 2005.
4. Liang, X. L., S.-S. Zhong, and W. Wang, "Tapered CPW-fed printed monopole antenna," *Microwave Opt. Tech. Lett.*, Vol. 48, No. 7, 1411–1413, 2007.
5. Lin, C.-C. and H.-R. Chuang, "A 3–12 GHz UWB planar triangular monopole antenna with ridged ground-plane," *Progress In Electromagnetics Research*, Vol. 83, 307–321, 2008.
6. Saleem, R. and A. K. Brown, "Empirical miniaturization analysis of inverse parabolic step sequence based UWB antennas," *Progress In Electromagnetics Research*, Vol. 114, 369–381, 2011.
7. Zhu, F., S.-C. Gao, A. T. S. Ho, T. W. C. Brown, J. Li, and J.-D. Xu, "Low-profile directional ultra-wideband antenna for see-through-wall imaging applications," *Progress In Electromagnetics Research*, Vol. 121, 121–139, 2011.
8. Chen, Z. and Y.-P. Zhang, "Effects of antennas and propagation channels on synchronization performance of a pulse-based ultra-wideband radio system," *Progress In Electromagnetics Research*, Vol. 115, 95–112, 2011.
9. Xu, H.-Y., H. Zhang, K. Lu, and X.-F. Zeng, "A holly-leaf-shaped monopole antenna with low RCS for UWB application," *Progress In Electromagnetics Research*, Vol. 117, 35–50, 2011.
10. Thomas, K. G. and M. Sreenivasan, "Printed elliptical monopole with shaped ground plane for pattern stability," *Electronic Lett.*, Vol. 45, No. 9, 445–446, 2009.
11. Yildirim, B. S., B. A. Cetiner, G. Roqueta, et al., "Integrated bluetooth and UWB antenna," *IEEE Antennas and Wireless Propag. Lett.*, Vol. 8, 149–152, 2009.
12. Liu, J. J., S. S. Zhong, and K. P. Esselle, "A printed elliptical monopole antenna with modified feeding structure for bandwidth enhancement," *IEEE Trans. Antennas Propag.*, Vol. 59, No. 2, 667–670, 2011.
13. Habib, M. A., A. Bostani, A. Djaiz, M. Nedil, M. C. E. Yagoub, and T. A. Denidni, "Ultra wideband CPW-FED aperture antenna with WLAN band rejection," *Progress In Electromagnetics Research*, Vol. 106, 17–31, 2010.
14. Hu, Y.-S., M. Li, G.-P. Gao, J.-S. Zhang, and M.-K. Yang, "A double-printed trapezoidal patch dipole antenna for UWB applications with band-notched characteristic," *Progress In Electromagnetics Research*, Vol. 103, 259–269, 2010.

15. Su, M., Y. Liu, S. Li, and C. Yu, "A compact open slot antenna for UWB applications with band-notched characteristic," *Journal of Electromagnetic Waves and Applications*, Vol. 24, No. 14–15, 2001–2010, 2010.
16. Barbarino, S. and F. Consoli, "UWB circular slot antenna provided with an inverted-L notch filter for the 5 GHz WLAN band," *Progress In Electromagnetics Research*, Vol. 104, 1–13, 2010.
17. Xie, L., Y.-C. Jiao, Y.-Q. Wei, and G. Zhao, "A compact band-notched UWB antenna optimized by a novel self-adaptive differential evolution algorithm," *Journal of Electromagnetic Waves and Applications*, Vol. 24, No. 17–18, 2353–2361, 2010.
18. Zhou, H. J., Q.-Z. Liu, Y.-Z. Yin, and W. B. Wei, "Study of the band-notch function for swallow-tailed planar monopole antennas," *Progress In Electromagnetics Research*, Vol. 77, 55–65, 2007.
19. Dissanayake, T. and K. P. Esselle, "Prediction of the notch frequency of slot loaded printed UWB antennas," *IEEE Trans. Antennas Propag.*, Vol. 55, No. 11, 3320–3325, 2007.
20. Wei, Y.-Q., Y.-Z. Yin, L. Xie, K. Song, and X.-S. Ren, "A novel band-notched antenna with self-similar flame slot used for 2.4 GHz WLAN and UWB application," *Journal of Electromagnetic Waves and Applications*, Vol. 25, No. 5–6, 693–701, 2011.
21. Yang, G., Q.-X. Chu, and Z.-H. Tu, "A compact band-notched UWB antenna with controllable notched bandwidths by using coupled slots," *Journal of Electromagnetic Waves and Applications*, Vol. 25, No. 14–15, 2148–2157, 2011.
22. Qu, X. A., S. S. Zhong, and W. Wang, "Study of the band-notch function for a UWB circular disc monopole antenna," *Microwave Opt. Technol. Lett.*, Vol. 48, No. 8, 1667–1670, 2006.
23. Xie, M., Q. Guo, and Y. Wu, "Design of a miniaturized UWB antenna with band-notched and high frequency rejection capability," *Journal of Electromagnetic Waves and Applications*, Vol. 25, No. 8–9, 1103–1112, 2011.
24. Deng, J. Y., Y. Z. Yin, J. Ma, and Q. Z. Liu, "Compact ultra-wideband antenna with dual band-notched characteristic," *Journal of Electromagnetic Waves and Applications*, Vol. 23, No. 1, 109–116, 2009.
25. Li, C.-M. and L.-H. Ye, "Improved dual band-notched UWB slot antenna with controllable notched bandwidths," *Progress In Electromagnetics Research*, Vol. 115, 477–493, 2011.

26. Zhang, M., X. Zhou, J. Guo, and W. Yin, "A novel ultrawideband planar antenna with dual band-notched performance," *Microwave Opt. Tech. Lett.*, Vol. 52, No. 1, 90–92, 2010.
27. Chu, Q. X. and Y. Y. Yang, "3.5/5.5 GHz dual band-notch ultrawideband antenna," *Electronic Lett.*, Vol. 44, No. 3, 172–174, 2008.
28. Anagnostou, D. E., S. Nikolaou, H. Kim, B. Kim, M. Tentzeris, and J. Papapolymerou, "Dual band-notched ultra-wideband antenna for 802.11a WLAN environments," *2007 IEEE Antennas and Propagation Society International Symposium*, 4621–4624, 2007.
29. Xia, Y.-Q., J. Luo, and D.-J. Edwards, "Novel miniature printed monopole antenna with dual tunable band-notched characteristics for UWB application," *Journal of Electromagnetic Waves and Applications*, Vol. 24, No. 13, 1783–1793, 2010.
30. Ni, T., W.-M. Li, Y.-C. Jiao, L.-S. Ren, and L. Han, "Novel compact UWB antenna with 3.5/5.5 GHz band-notched characteristics," *Journal of Electromagnetic Waves and Applications*, Vol. 25, No. 16, 2212–2221, 2010.
31. Wang, M., J.-X. Xiao, and S. Wang, "Study of a dual-band notched wideband circular slot antenna," *Journal of Electromagnetic Waves and Applications*, Vol. 24, No. 17–18, 2445–2452, 2010.
32. Li, Z.-Q., C.-L. Ruan, and L. Peng, "Design and analysis of planar antenna with dual WLAN band-notched for Integrated Bluetooth and UWB applications," *Journal of Electromagnetic Waves and Applications*, Vol. 24, No. 13, 1817–1828, 2010.
33. Ren, L.-S., F. Li, J.-J. Zhao, G. Zhao, and Y.-C. Jiao, "A novel compact UWB antenna with dual band-notched characteristics," *Journal of Electromagnetic Waves and Applications*, Vol. 24, No. 11–12, 1521–1529, 2010.
34. Nikolaou, S., M. Davidovic, M. Nikolic, and P. Vryonides, "Triple notch UWB antenna controlled by three types of resonators," *2011 IEEE International Symposium on Antennas and Propagation (APSURSI)*, 1478–1481, 2011.
35. Nguyen, T. D., D. H. Lee, and H. C. Park, "Design and analysis of compact printed triple band-notched UWB antenna," *IEEE Antennas and Wireless Propag. Lett.*, Vol. 10, 403–406, 2011.
36. Liao, X.-J., H.-C. Yang, N. Han, and Y. Li, "A semi-circle-shaped aperture UWB antenna with triple band-notched characteristics," *Journal of Electromagnetic Waves and Applications*, Vol. 25, No. 2–3, 257–266, 2011.